Elasticity, internal excitation, fragmentation, and charge transfer during grazing scattering of fast fullerenes from a KCl(001) surface

S. Wethekam, J. Merck, M. Busch,* and H. Winter
Institut für Physik, Humboldt-Universität zu Berlin, Newtonstrasse 15, D-12489 Berlin, Germany
(Received 28 October 2010; published 25 February 2011)

C_{60}^+ and C_{70}^+ fullerenes with keV energies are scattered under grazing polar angles of incidence from an atomically clean and flat KCl(001) surface. For this model system of molecule surface interactions, the elastic properties of the fullerenes in front of the surface are studied by polar angular distributions. From the analysis of fragment spectra, the internal excitations of scattered molecules are deduced and excitation mechanisms are identified. Charge fractions indicate a kinematically induced neutralization of the fullerenes. Via an analysis of negatively charged fragments, the transition from a "soft" scattering event with intact outgoing fullerenes to postcollision multifragmentation is analyzed. The data are compared to three-dimensional molecular dynamics simulations based on empirical bond-order potentials.

DOI: 10.1103/PhysRevB.83.085423 PACS number(s): 79.20.Rf, 34.35.+a, 79.60.Bm

I. INTRODUCTION

The interaction of atoms and molecules with solid surfaces plays an important role in many fields such as surface analysis, heterogenous catalysis, secondary ion mass spectrometry, low-energy ion scattering, scanning tunneling microscopy, plasma wall interactions, and molecular electronics. During the last decades, a large body of work has been devoted to studies on the basic mechanisms.[1–7] In this respect, scattering of hyperthermal atoms and molecules from solid surfaces has proven to be a valuable experimental tool. Whereas many aspects of the interaction of atomic projectiles with solid surfaces have been worked out in detail, studies involving molecules are rather rare and suffer from an enhanced complexity introduced by internal degrees of freedom of the projectiles.[1,2,5,6] Due to their symmetrical shape, stability, and well-known physical properties, and the wide range of possible applications of carbon nanostructures,[3,4,8,9] fullerenes represent an ideal candidate for exploring molecule/cluster surface interactions.[2]

Early studies on fullerene surface scattering in the hyperthermal regime are reviewed in Refs. 2 and 10. Here, we focus on work closely related to our studies only. Beck *et al.* have scattered C_{60}^+ and larger fullerenes with energies of a few hundred electron volts under an angle of incidence of $\Phi_{in} = 45^\circ$ with respect to the target surface from clean and adsorbate-covered graphite surfaces. The kinetic energy of outgoing clusters was greatly reduced, to about 20 eV. From fragment size distributions, an energy transfer to internal degrees of freedom of 30% (10% for adsorbate-covered surfaces) and an onset for shattering of the molecules at the surface of about 400 eV were derived. To reduce the energy transfer to the surface, studies for a near-grazing angle of incidence of $\Phi_{in} = 15^\circ$ were performed, but the energy transfer to the surface was still considerable.[11] The analysis of charge states revealed a neutralization probability of 99% and fractions of negative ions of some 10^{-3} for the clean surface.[12]

The deposition of carbon, angular and energy distributions, and internal excitations for scattering of neutral C_{60} molecules with energies of some tens of electron volts from a polycrystalline Ni surface was analyzed by Kolodney *et al.*[13] Kinetic energy losses of 40%–85% were observed, where 2% of the kinetic energy was transferred to internal excitations, only. From the analysis of image charge effects on angular distributions and ion fractions, an effective distance for the formation of negative ions of about 13 Å and negative ion yields of 0.1%–0.5% were derived.[14,15] The stability of the molecules was studied for scattering from a gold surface at highger projectile energies, of some hundreds of electron volts, as a function of the angle of incidence Φ_{in}. Via an analysis of the energy distributions for small outgoing C_n^- fragments ($n = 2$–12), a transition from "during-collision" to "postcollision" multifragmentation was observed and modeled by treating the fragmenting cluster as a hot "gas" of C_n fragments.[16,17]

A quantitative interpretation of studies on fullerene surface collisions under large-angle impact is complex. The pronounced deformation of the surface has a strong impact on the outcome of the scattering process, which makes it virtually impossible to disentangle properties of the fullerene, the surface, or their interaction in many cases. First studies under grazing incidence, that is, in the regime of surface channeling[1,18] for polar angles of about 1° incidence, have been reported by Kimura *et al.*[19–21] These angles are sufficiently small to guarantee negligible nuclear energy losses (except for the excitation of optical phonons for charged projectiles). C_{60}^+ and C_{60}^0 projectiles of 1–3 keV with energies of up to 20 eV for the motion normal to the surface were scattered elastically from a KCl(001) surface, while the total losses of kinetic energy amounted up to about 100 eV (motion parallel to surface). These were attributed to the excitation of optical phonons and internal degrees of freedom of the molecules but were not understood on a quantitative level. From fractions of surviving molecular ions and shifts of angular distributions for incident neutral and charged molecules, the neutralization rate and the level shift of the highest-occupied molecular orbital of the fullerenes in front of the surface were derived, respectively. Recently, resonant coherent excitation[22–25] has been reported for C_{60} scattered from KCl(001) along specific azimuthal directions.[20,26]

In our previous works, we have studied the interaction of C_{60} molecules with two metal surfaces with pronounced differences in electronic structure, Al(100) and Be(0001), in the regime of surface channeling with kilo–electron volt

energies and grazing polar angles of about 1° incidence.[27–30] We focused on the elastic properties and the internal excitation of the molecules as well as on electron capture. For normal energies of some electron volts, the molecules were scattered elastically, whereas for normal energies, higher than about 10 eV, an increasing fraction, up to about 90% (at 40 eV), of the normal energy was transferred to internal excitations. Molecular dynamics simulations reproduced the main characteristics of the normal energy loss and internal excitation on a qualitative level. Charged C_{60}^{2+} and C_{60}^{+} molecules were efficiently neutralized at the surface. From shifts of polar angular distributions for scattering of molecules in different charge states due to image charge attraction prior to neutralization, effective distances for electron capture in good accord with a classical over-barrier model by Zettergren *et al.*[31] were derived. The pronounced suppression of charge transfer for atoms in front of surfaces with a projected band gap[1,5] was not observed for the fullerene, which was explained by a simple model and attributed to the extended shape of the molecule. Recently, we have investigated the scattering from LiF(001), an insulator with a pronounced band gap, and found complete suppression of charge transfer for C_{60}^{+} molecules and an efficient "dynamical" excitation mechanism, which was interpreted in terms of resonant coherent excitation.[32]

Here, we study the elasticity, internal excitation, fragmentation, and charge transfer of C_{60} and C_{70} molecules during grazing scattering from a KCl(001) surface. Despite also being a large band gap insulator, the interaction of fullerenes with KCl(001), especially the charge transfer, is different from that with LiF(001), as the highest occupied molecular orbital (HOMO) of neutral fullerenes is nearly degenerate with the valence band maximum of KCl(001) (separation of some 0.1 eV only). To demonstrate the applicability of our results to other fullerenes, we extended our studies to C_{70}. Furthermore, we analyze the transition from the low-energy regime, where the molecules are scattered intact from the surface, to the high-energy regime, where multifragmentation phenomena come into play. Our work provides complimentary information to the studies by Kimura *et al.*[19–21] for the same system, which were performed at lower energies.

II. EXPERIMENTAL SETUP

In our experiments, we have scattered C_{60}^{+} and C_{70}^{+} molecules with energies from $E = 5$ keV up to some 10 keV under grazing polar angles of incidence of $\Phi_{in} = 0.5$–$3.5°$ from an atomically clean and flat KCl(001) surface. Scattering proceeds in the surface channeling regime,[1,18] where the motions parallel and normal to the surface are widely decoupled. Whereas the parallel motion takes place at kilo–electron volt energies, $E_{\parallel} = E\cos^2\Phi_{in} \approx E$, the interaction with the surface is governed by the slow normal motion with an energy orders of magnitude lower, $E_{\perp}^{in} = E\sin^2\Phi_{in} \sim 10^{-3}E$, that is, in the regime of electron volts.

The fullerene beams are produced via evaporation of fullerene powder (SES Research, Houston, TX, USA) in Ar gas using an electron cyclotron resonance ion source (Nanogan; Pantechnik; Bayeux, France). The projectiles are mass-separated in a 90° magnet after a first acceleration stage to 2.8 kV. Afterward, the fullerenes are accelerated up to 100 keV and pass a system of slits, which separate two differential pumping stages, before impacting the surface located in an ultrahigh-vacuum) chamber with a base pressure of some 10^{-11} mbar. The residual beam divergence amounts to about 0.03°. Charge states and charged fragments of scattered molecules are dispersed by electric fields and detected with a position-sensitive microchannel plate (MCP) detector (DLD40; Roentdek; Kelkheim-Ruppertshain, Germany). Variations of the detection efficiency across the active area of the MCP are corrected by wobbling a fullerene beam. The grazing polar angles of incidence Φ_{in} are determined with 2.8-keV Ar^0 atoms, which are specularly reflected from the surface. The surface is prepared by cycles of grazing sputtering with 25-keV Ar^+ ions and subsequent annealing to 400°C. During measurements, the surface is kept at a temperature of 200°C to avoid surface charging. The quality of the surface is monitored by ion beam techniques, such as ion beam triangulation and the shape of polar angular distributions.[1,33] For more details on the experimental setup, we refer to Refs. 1 and 27.

III. ELASTICITY, INTERNAL EXCITATION, AND NEUTRALIZATION

In Fig. 1, we show raw data for polar angular distributions recorded with the MCP detector (normalized intensity encoded in color scale) for scattering of C_{70}^{+} ions with indicated energies $E = 5$–30 keV [Figs. 1(a)–1(d)] under a grazing angle of incidence $\Phi_{in} = 2.2°$ along a high-indexed (random) direction of the KCl(001) surface. The vertical axis corresponds to the polar exit angle Φ_{out}. To separate different charge states, the scattered projectiles pass a slit, which limits the azimuthal deflection angle (y direction) to ±0.25°, and electric field plates. Positively charged projectiles are deflected to the

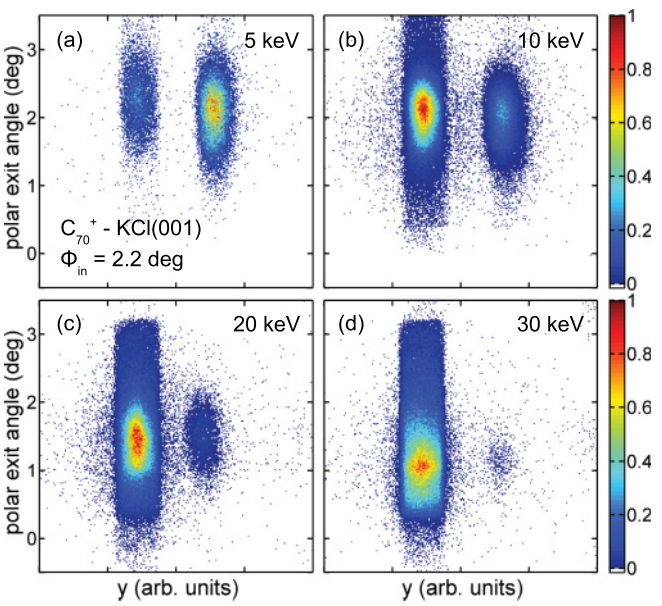

FIG. 1. (Color online) Polar angular distributions recorded with the MCP detector (normalized intensity encoded in color scale) for scattering of C_{70}^{+} ions with energies indicated under a grazing angle of incidence $\Phi_{in} = 2.2°$ along the high-indexed (random) direction of KCl(001). Distributions of (left) neutral projectiles and (right) positively charged projectiles.

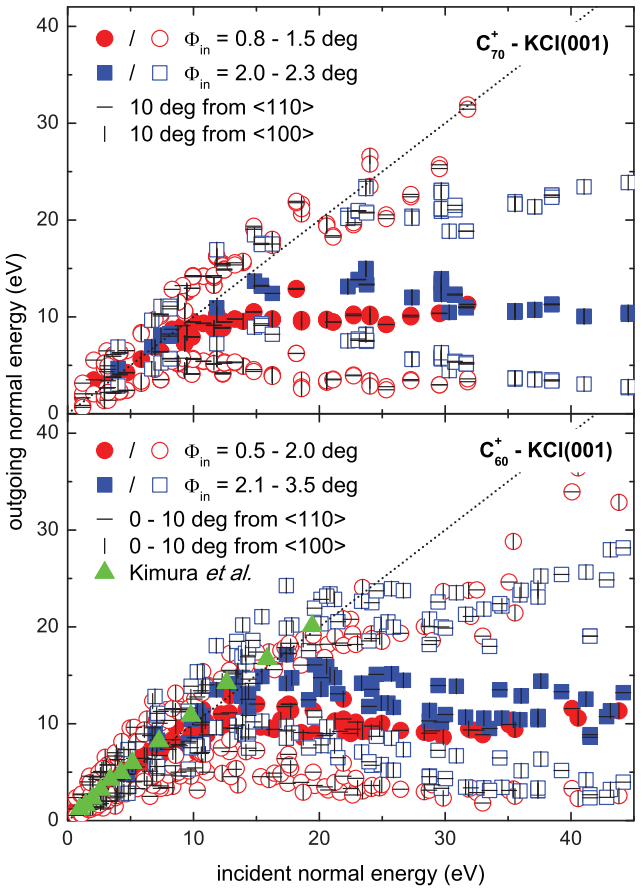

FIG. 2. (Color online) Outgoing normal energy $E_\perp^{\text{out}}$ as a function of the incident normal energy $E_\perp^{\text{in}}$ for maxima (full symbols) and half-maximum positions (open symbols) of polar angular distributions for scattering of C_{70}^+ (top) and C_{60}^+ molecules (bottom) from KCl(001) under the indicated angles of incidence Φ_{in} and indicated azimuthal orientations with respect to low-indexed directions of the surface. Filled triangles: experimental data of Kimura *et al.*[19,21] for scattering of $E = 3$ keV C_{60}^+ from KCl(001). Dotted curves: specular reflection.

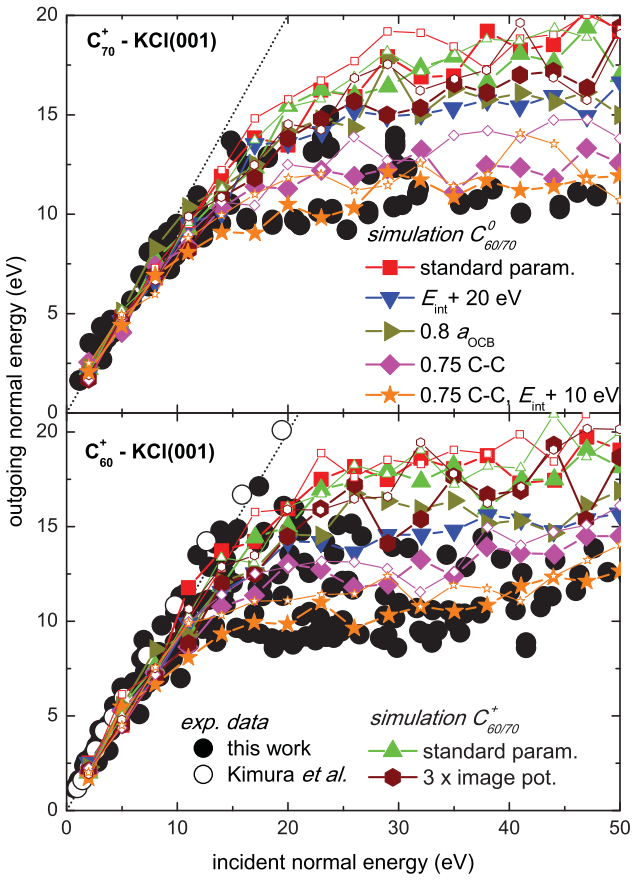

FIG. 3. (Color online) Outgoing normal energy $E_\perp^{\text{out}}$ as a function of the incident normal energy $E_\perp^{\text{in}}$ derived from maxima of angular distributions for scattering of C_{70}^+ (top) and C_{60}^+ (bottom) from KCl(001). Filled and open circles: experimental data from Fig. 2 and from Kimura *et al.*,[19,21] respectively. Thin curves with open symbols and thick curves with filled symbols: classical 3D trajectory simulations based on BOP by Tersoff[37] and by Erhart and Albe,[38] respectively, for different indicated parameter sets. For details see the text.

right. Therefore, the polar angular distributions of neutral and positively charged projectiles are detected in the left and right bars, respectively.

At $E = 5$ keV, the fullerenes are scattered nearly elastically [Fig. 1(a)], whereas with increasing energy E the polar exit angle Φ_{out} is reduced and the fullerenes are scattered subspecularly [Figs. 1(c) and 1(d)]. Except for the lowest energy, where the image charge potential results in a small shift in the angular distributions for both charges,[28,30] the angular distributions for neutral and charged outgoing projectiles coincide. At low energies, predominantly positively charged projectiles are observed, whereas neutral projectiles dominate the charge state distribution at larger energies.

A. Elasticity

For a more detailed discussion of the elasticity, outgoing normal energies $E_\perp^{\text{out}} = E \sin^2 \Phi_{\text{out}}$ as a function of incident normal energy $E_\perp^{\text{in}}$ derived from the maxima [half-maximum positions] of polar angular distributions for scattering of C_{70}^+ (top) and C_{60}^+ molecules (bottom) from KCl(001) under the indicated angles of incidence Φ_{in} and azimuthal orientations are given in Fig. 2 by filled [open] symbols. The data of Kimura *et al.*[19,21] for impact of $E = 3$ keV C_{60}^+ on KCl(001) is shown by filled triangles. The results for both fullerenes are similar and do not depend on the azimuthal orientation of the surface. For normal energies $E_\perp^{\text{in}} \leqslant 12$ eV, the molecules are reflected elastically, whereas at higher normal energies $E_\perp^{\text{in}} \geqslant 12$ eV, subspecular scattering is observed with an outgoing normal energy $E_\perp^{\text{out}} \approx 12$ eV independent of the incident normal energy $E_\perp^{\text{in}}$.

In the region of subspecular scattering, the data show a slight dependence on the angle of incidence Φ_{in}, with a tendency toward lower outgoing normal energies for smaller Φ_{in} or, equivalently, toward higher energies $E \approx E_\parallel$ for motion parallel to the surface. The data of Kimura *et al.*,[19,21] shown in the lower panels in Figs. 2 and 3, are consistent with our work, since their measurements were performed at an energy $E = 3$ keV, which is lower than the energies $E \geqslant 5$ keV used in our experiments. Furthermore, the work by Kimura *et al.* was restricted to an incident normal energy $E_\perp^{\text{in}}$ lower than 20 eV. The outgoing normal energies for KCl(001) are

somewhat lower than for LiF(001),[32] an insulator with a more pronounced band gap, and higher than for Al(001).[27,29] As the valence band maximum of KCl(001)[34,35] is located only about 0.5 eV below the HOMO of the fullerenes,[8] a kinematically assisted hybridization[1,3,36] that influences the elastic constants of the fullerene is a possible explanation. This is consistent with our simulations and our data on charge transfer, where kinematic effects are also observed (see below).

To analyze the elastic behavior of the fullerenes in more detail, we compare the experimental outgoing normal energies $E_\perp^{\text{out}}$ as a function of the incident normal energy $E_\perp^{\text{in}}$ (filled circles) with classical 3D trajectory simulations for different parameters in Fig. 3. In the simulations, Newton equations of motion for the fullerene atoms and the target atoms are solved numerically using a fourth-order Runge-Kutta method. For the interaction of the C atoms of the fullerene, we use the well-established empirical bond-order potential (BOP) of Tersoff[37] (thin curves with open symbols) and a recent optimized variant by Erhart and Albe[38] (thick curves with filled symbols). For fullerene ions, the Coulomb interaction is included for a charge evenly distributed over the C atoms. At the interaction energies of up to several tens of electron volts relevant here, polarization effects[28,31] can be safely neglected. The fullerene-surface interaction is modeled by a Molière potential with modified Firsov screening length a_{OCB} as proposed by O'Connor and Biersack[39] (OCB potential) and, for charged fullerenes, the classical image charge potential. The internal vibrational excitation of the incident molecules of 35 and 40 eV for C_{60} and C_{70} (see Fig. 5 and Refs. 27 and 29), respectively, is distributed over the vibrational degrees of freedom of incident molecules and thermalized during a number of oscillation periods prior to the surface impact. Uncorrelated thermal displacements of target atoms are included in the framework of the Debye model for Debye temperatures from Ref. 40. Each data point in Fig. 3 is based on 20 trajectories. For each trajectory, the fullerene is randomly oriented and placed with respect to a unit cell of the surface. For more details on the simulations, we refer to Refs. 27,29, and 41.

Based on these parameters, the outgoing normal energies $E_\perp^{\text{out}}$ at high $E_\perp^{\text{in}}$ are overestimated. The results for the BOPs by Tersoff[37] and Erhart *et al.*[38] coincide for both neutral (curves with squares) and positively charged (curves with upward triangles) C_{60} and C_{70} molecules. For a more detailed analysis, we present calculations for different interactions of the fullerene with the surface and modified BOPs. The charge of the fullerene is not responsible for the discrepancy, as a three times stronger image charge potential does not result in any change (curves with hexagons). The same holds for internal excitations of the incident molecules and the repulsive part of the interaction potential with the surface, where an increase in the internal energy by 20 eV (curves with downward triangles) or a reduction in the screening length by a factor of 0.8 (curves with right-pointing triangles) do not affect the outgoing normal energy, respectively.

In good accord with a similar analysis for the system C_{60}–Al(001),[27,29] where the interaction of the fullerene with the surface was varied over a wide range including physically unreasonable parameters, we conclude that the elastic properties of the fullerene itself determine the outgoing normal energy $E_\perp^{\text{out}}$. A reduction of the BOPs by a factor of 0.75 (curves with diamonds) yields quantitative agreement with our experimental data also for a slightly enhanced internal energy of the fullerenes observed for high normal energies $E_\perp^{\text{in}}$ and small angles of incidence Φ_{in} (curves with stars; see Fig. 5 and Sec. III B). This modification of the BOPs is in good accord with our analysis of multifragmentation phenomena in Sec. IV and may be interpreted as a deficiency of the BOPs or as an influence of a kinematically assisted hybridization of the electronic states of the fullerenes with the valence band of KCl(001) on the elastic properties of fullerenes.[1,3,36,42]

B. Internal excitation

For normal energies $E_\perp^{\text{in}} \leqslant 30$ eV, shattering of molecules at the KCl(001) surface is not expected.[16,17,27,43,44] This is in accord with the molecular dynamics simulations discussed above, the analysis of multifragmentation phenomena in Sec. IV, and the bimodal fragment size distributions discussed in this section. The molecules leave the surface intact, but internally excited. The internal energy is dissipated via the delayed evaporation of neutral C_2^0 fragments or delayed electron emission,[2,10,45] so that the former can be inferred from fragment size distributions. For ion fractions larger than a few percent[27,45] (most of the fragment spectra discussed in this section; cf. Figs. 5 and 7), the bimodal mass spectra of positive fragments are dominated by delayed C_2^0 emission from a positive $C_{60/70}^+$ precursor.

In the inset in Fig. 4, we show typical raw data for positive fragments for C_{70}^+ impacting on KCl(001) with an energy $E = 50$ keV under an angle of incidence $\Phi_{\text{in}} = 0.9°$. The spectrum is recorded via deflection of scattered projectiles from the maximum of the polar angular distribution in an electric field. The projection on the deflection axis is shown in Fig. 4 (solid curve). To derive the internal energy

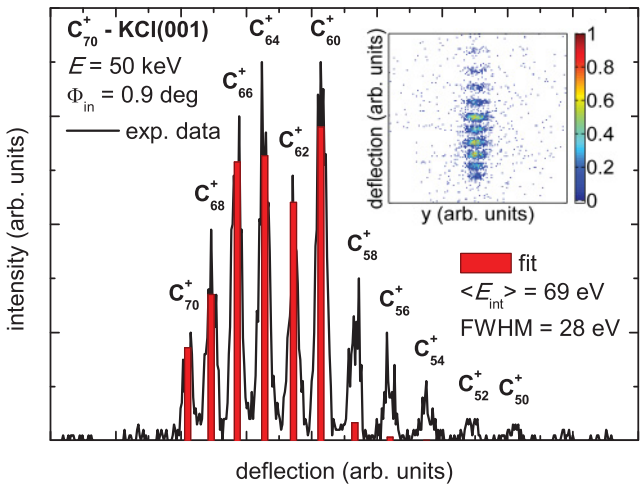

FIG. 4. (Color online) Solid curve: fragment size distribution measured via deflection of projectiles from the maximum of the polar angular distribution in the electric field for scattering of 50-keV C_{70}^+ from KCl(001) under $\Phi_{\text{in}} = 0.9°$. Bars: fit of fragment spectrum based on theoretical model for delayed C_2^0 emission. Inset: Raw data as recorded with MCP detector. For details see text.

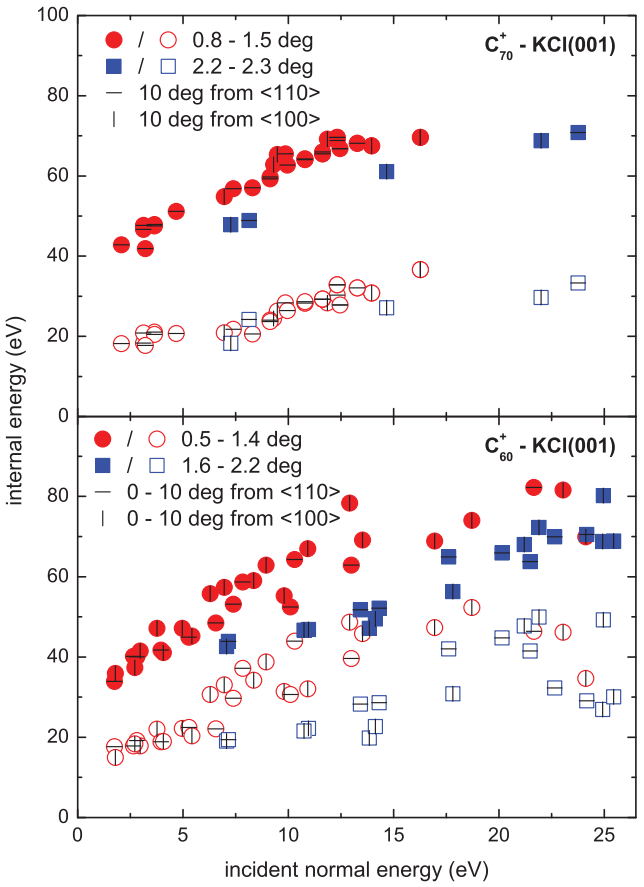

FIG. 5. (Color online) Mean energies $\langle E_{\rm int}\rangle$ (filled symbols) and FWHM (open symbols) of internal energy distributions derived from positive fragment spectra as a function of incident normal energy $E_\perp^{\rm in}$ for scattering of C_{70}^+ (upper panel) and C_{60}^+ (lower panel) under the indicated polar angles of incidence $\Phi_{\rm in}$ along the indicated azimuthal directions from KCl(001). For details see the text.

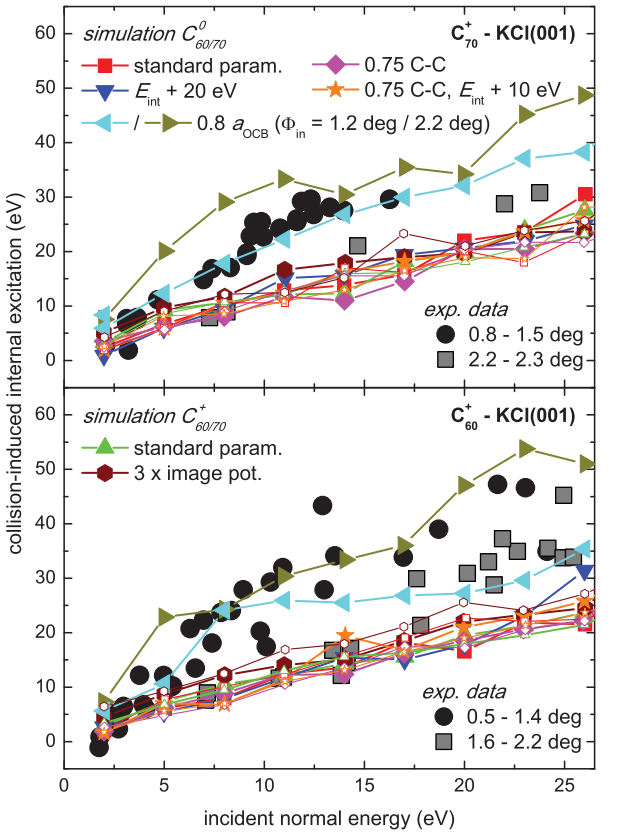

FIG. 6. (Color online) Collision-induced internal excitation as a function of incident normal energy $E_\perp^{\rm in}$ for scattering of C_{70}^+ (upper panel) and C_{60}^+ (lower panel) from KCl(001) under indicated polar angles of incidence $\Phi_{\rm in}$. Symbols: experimental data from Fig. 5. Classical 3D trajectory simulations based on BOP by Tersoff[37] (thin curves with open symbols) or Erhart and Albe[38] (thick curves with filled symbols) for different indicated parameter sets. For details see the text.

distribution for scattered fullerenes, the data are fitted with a Gaussian distribution of internal energies of fullerenes leaving the surface using an established Arrhenius representation of the rates for delayed C_2^0 emission for parameters from Concina *et al.*[45] This yields a quantitative reproduction (bars in Fig. 4) of the experimental fragment size distribution for a mean internal energy of $\langle E_{\rm int}\rangle = 69$ eV and a full width at half-maximum (FWHM) of 28 eV of the internal energy distribution. For more details on the analysis, we refer to Ref. 27.

Mean energies $\langle E_{\rm int}\rangle$ (filled symbols) and FWHM (open symbols) of internal energy distributions derived from positive fragment spectra as a function of incident normal energy $E_\perp^{\rm in}$ for scattering of C_{70}^+ (upper panel) and C_{60}^+ (lower panel) under the indicated polar angles of incidence $\Phi_{\rm in}$ along specific azimuthal directions from KCl(001) are given in Fig. 5. Again, similar excitations as well as no azimuthal dependencies are observed for both fullerenes. The mean internal energy $\langle E_{\rm int}\rangle$ and the FWHM show an almost-linear dependence on the incident normal energy $E_\perp^{\rm in}$, with somewhat higher internal excitations for smaller angles of incidence $\Phi_{\rm in}$. This behavior is intermediate to the interaction of C_{60}^+ with Al(100) and LiF(001), where the internal excitation is given by the normal energy loss $E_\perp^{\rm loss} = E_\perp^{\rm in} - E_\perp^{\rm out}$[27,29] or shows a more pronounced dependence on the angle of incidence $\Phi_{\rm in}$,[32] respectively.

In Fig. 6, the experimental mean internal excitation energies $\langle E_{\rm int}\rangle$ corrected for the internal excitation of the incident clusters [35 eV (40 eV) for C_{60} (C_{70})] ("collision-induced internal excitation"), obtained via extrapolation of the internal energies in Fig. 5 to $E_\perp^{\rm in} = 0$, as a function of the incident normal energy $E_\perp^{\rm in}$ (symbols) are compared to results from 3D trajectory simulations (curves with symbols) for parameter sets discussed in Sec. III A. The simulations reproduce the general trends but underestimate the internal excitation, especially for small angles of incidence (filled circles). This can be compensated via an enhancement of the corrugation of the surface potential by reducing the screening length $a_{\rm OCB}$ by a factor of 0.8 (curves with leftward- and rightward-pointing triangles) but results in another angular dependence with higher excitations for larger angles of incidence $\Phi_{\rm in}$ (curves with rightward-pointing triangles).

The internal excitations are not reproduced by our classical trajectory simulations. Therefore, we conclude an additional excitation of the electronic system not included in our model. As discussed for energy loss and fragmentation during grazing scattering of C_{60}^+ molecules from KCl(100) by

Matsushita *et al.*,[20,26] a possible mechanism might be resonant coherent excitation,[1,22–25] an excitation related to the oscillating electric field in the rest frame of the molecule due to the point charge lattice at the surface. The frequency of this field is in the near infrared and, therefore, in the region of the HOMO-LUMO gap (LUMO: lowest unoccupied molecular orbital) of the neutral molecule, so that it is present for the charged molecule, only. This explains our recent observation of even stronger excitations of fullerenes during grazing scattering from LiF(001),[32] where the neutralization is suppressed completely, whereas for KCl(001), major fractions of fullerenes are neutralized at high normal energies (see Sec. III C).

C. Neutralization

In Fig. 7, we show measured positive ion fractions P^+ (filled symbols) as a function of incident normal energy $E_\perp^{\text{in}}$ for scattering of C_{70}^+ (upper panel) and C_{60}^+ (lower panel) molecules under the indicated polar angles of incidence Φ_{in} along the indicated azimuthal directions from KCl(001). Whereas no azimuthal dependence is observed, the ion fractions for different angles of incidence differ by up to an order of magnitude.

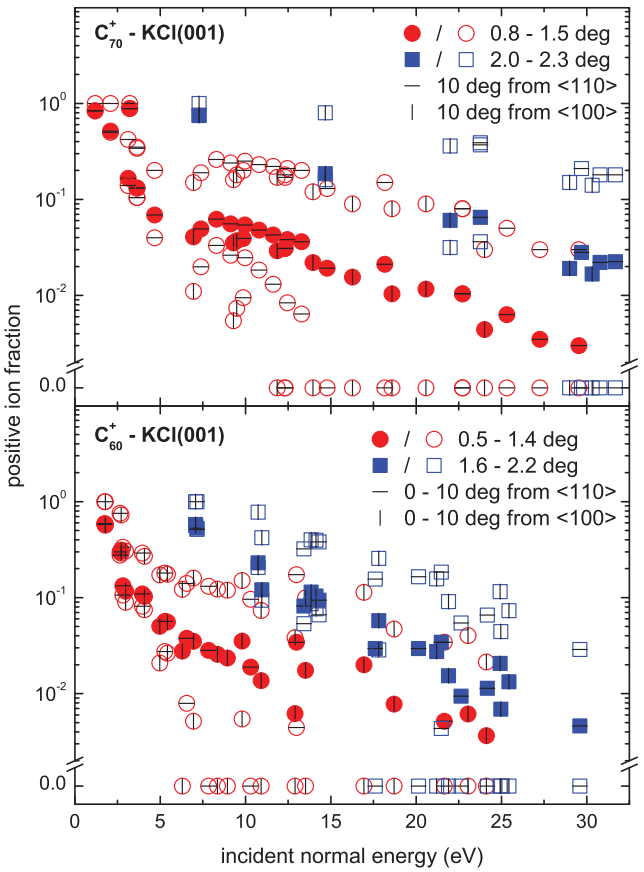

FIG. 7. (Color online) Experimental positive ion fractions P^+ (filled symbols) as a function of incident normal energy $E_\perp^{\text{in}}$ for scattering of C_{70}^+ (upper panel) and C_{60}^+ (lower panel) molecules under the indicated polar angles of incidence Φ_{in} along indicated azimuthal directions from KCl(001). Open symbols: upper and lower limits for the fractions of positive ions leaving the surface P_{surf}^+. For details see the text.

Via delayed C_2^0 and electron emission processes, the outcome of the fullerene surface interaction is modified during the flight of scattered molecules to the detector. Therefore, the measured ion fractions do not directly reflect the fractions P_{surf}^+ of fullerene ions leaving the surface. However, the mean number of emitted C_2^0 molecules can be determined from measured fragment size distributions (see Sec. III B) and the delayed ionization probability for neutral fullerenes is less than 3%.[2,10,27,45] Therefore, lower [upper] limits for the ion fractions P_{surf}^+ determined by the scattering process with the surface (open symbols) can be derived from measured ion fractions P^+ and fragment size distributions assuming a relative detection efficiency for C_2^0 molecules with respect to large fullerene molecules of zero [one] in conjunction with a delayed ionization probability of 3% [0%].

Despite these uncertainties, our data show an almost-complete survival of incident ions at low energies as already reported by Kimura *et al.*[19–21] for C_{60}^+ scattered from KCl(001). At larger incident normal energies $E_\perp^{\text{in}}$ an efficient neutralization is observed with smaller positive ion fractions for smaller angles of incidence (circles) at the same $E_\perp^{\text{in}}$. The incident normal energy determines the distance of closest approach to the surface and the interaction time. As the same normal energy for smaller angles of incidence is achieved at higher velocities for the motion parallel to the surface, the angular dependence is a clear-cut indication of a kinematically assisted charge transfer.[1,36] This is in accord with the small energy defect of the valence band maximum of KCl(001) and the HOMO of the fullerenes of 0.5 eV.[8,34] A more detailed theoretical analysis is beyond the scope of this work.

IV. NEGATIVE ION FORMATION AND POSTCOLLISION MULTIFRAGMENTATION

Aside from resonant one-electron tunneling and due to the high electron affinities of the fullerenes,[8] our data are also in accord with a second charge transfer mechanism, the negative ion formation via double-electron capture from adjacent halide sites.[46] This process was reported for atomic projectiles with a high electron affinity. At the internal excitations of fullerenes in our experiments (see Sec. III B), the negative charge of fullerenes leaving the surface is quenched by delayed electron emission on a time scale of about 10^{-10} s.[47] Therefore, only neutral fullerenes will reach the detector (flight time of some microseconds).

However, in the so-called postcollision multifragmentation regime at high energies, the detachment of the negative charge can be avoided by a multiparticle breakup of the fullerene prior to electron detachment. Then, small negatively charged C_n ($n \approx 2$–20) fragments, which exhibit large electron affinities,[48] may be detected. This process has been reported by Kaplan *et al.*[16,17] for scattering of C_{60} molecules with energies of some 100 eV from a gold surface under large angles of incidence. At grazing incidence, that is, for a negligible energy transfer to the surface, this process has not been observed so far and a normal energy threshold of about 180 eV has been predicted.[44] In the following, we discuss our data on postcollision multifragmentation of C_{60} and C_{70} molecules

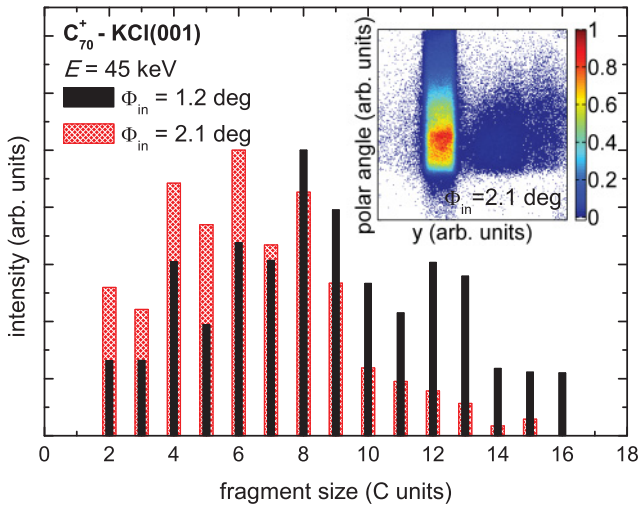

FIG. 8. (Color online) Thin(thick) bars: fragment size distributions of small, negatively charged C_n^- fragments for scattering of C_{70}^+ molecules with energy $E = 45$ keV under $\Phi_{in} = 1.2°(2.2°)$ from KCl(001). Inset: raw data for polar angular distributions as recorded with the MCP detector for scattering of C_{70}^+ molecules with $E = 45$ keV under $\Phi_{in} = 2.1°$ from KCl(001). Left bar: neutral projectiles. Negatively charged small C_n^- fragments deflected to the right. Distributions for different n overlaps.

during grazing scattering from KCl(001), which, due to the internal excitation of the incident molecules, shows a normal energy threshold of only about 20 eV.

In Fig. 8, we present fragment size distributions of small, negatively charged C_n^- fragments for scattering of C_{70}^+ molecules with energy $E = 45$ keV under polar angles of incidence of $\Phi_{in} = 1.2°$ (thin bars) and $\Phi_{in} = 2.2°$ (thick bars) from KCl(001). C_n^- fragments in the range $n = 2$–16 are observed, with a more pronounced fragmentation for a larger angle of incidence (higher normal energy) and a modulation related to the electron affinities of the clusters,[48] in good accord with the data of Kaplan *et al.*[16,17] The inset in Fig. 8 shows raw data for polar angular distributions as recorded with the MCP detector for scattering of C_{70}^+ molecules with $E = 45$ keV under $\Phi_{in} = 2.1°$ from KCl(001). The left bar corresponds to neutral projectiles, whereas the negative fragments are deflected to the right side. Different sizes n are not resolved under these conditions. Nevertheless, one can conclude that the polar angular distribution for small fragments, which are more strongly deflected, is broader than for larger fragments. The distributions for neutral molecules and negative fragments are well-defined and similar, which serves as a first hint for an intact fullerene as a precursor and, therefore, postcollision multifragmentation.[16,17]

For a quantitative discussion, measured negative ion fractions as function of the incident normal energy $E_\perp^{in}$ for scattering of C_{70}^+ (upper panel) and C_{60}^+ (lower panel) molecules under indicated polar angles of incidence Φ_{in} and azimuthal directions from KCl(001) (symbols) are compared to results from 3D trajectory simulations for the indicated parameters and angles of incidence (curves with symbols) in Fig. 9. Again, the results for both fullerenes are comparable and independent of the azimuthal orientation of the surface. They

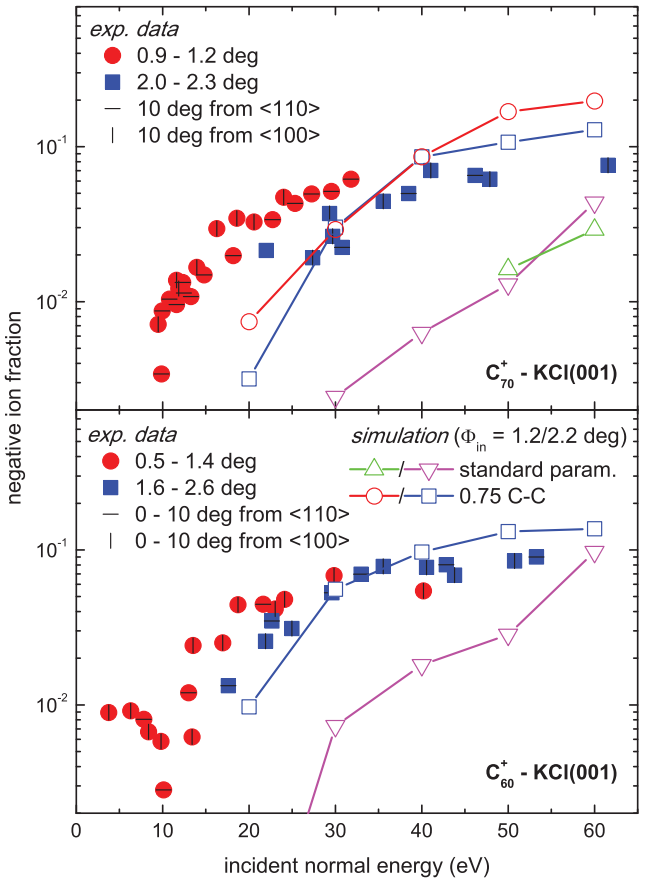

FIG. 9. (Color online) Measured negative ion fractions as a function of incident normal energy $E_\perp^{in}$ for scattering of C_{70}^+ (upper panel) and C_{60}^+ (lower panel) molecules under indicated polar angles of incidence Φ_{in} and azimuthal directions from KCl(001) (symbols) compared to results from 3D trajectory simulations for indicated angles and parameters (curves with symbols). For details see text.

show a slight dependence on the angle of incidence, only with larger negative ion fractions for smaller angles. For normal energies $E_\perp = 10$–30 eV, the negative ion fractions increase exponentially and saturate at a value of nearly 10% for normal energies $E_\perp \geqslant 40$ eV.

The 3D trajectory simulations are detailed in Sec. III A. In Fig. 10, we show snapshots for typical simulated trajectories. In the simulations, no shattering at the surface is observed for the whole range of impact parameters of our experiments. The molecules leave the surface intact [Fig. 10(a)] or as a single cluster with a few broken bonds [Fig. 10(b)]. Only defects at the surface such as steps may induce shattering of the fullerenes at the surface [Fig. 10], which then results in poor broad angular distributions [inset in Fig. 10(c)]. For normal energies $E_\perp \geqslant 30$ eV, the measured negative ion fractions in Fig. 9 for different angles Φ_{in} as well as the simulated fractions coincide. As for the same normal energy $E_\perp^{in}$, the angle Φ_{in} determines the length of the trajectory, which is proportional to the probability one of hitting a surface defect. A relevant role of surface defects on the experimental ion fractions can be ruled out in the region of higher normal energies.

In the simulations, we assume a conversion efficiency to negative ions of one during scattering from the surface.

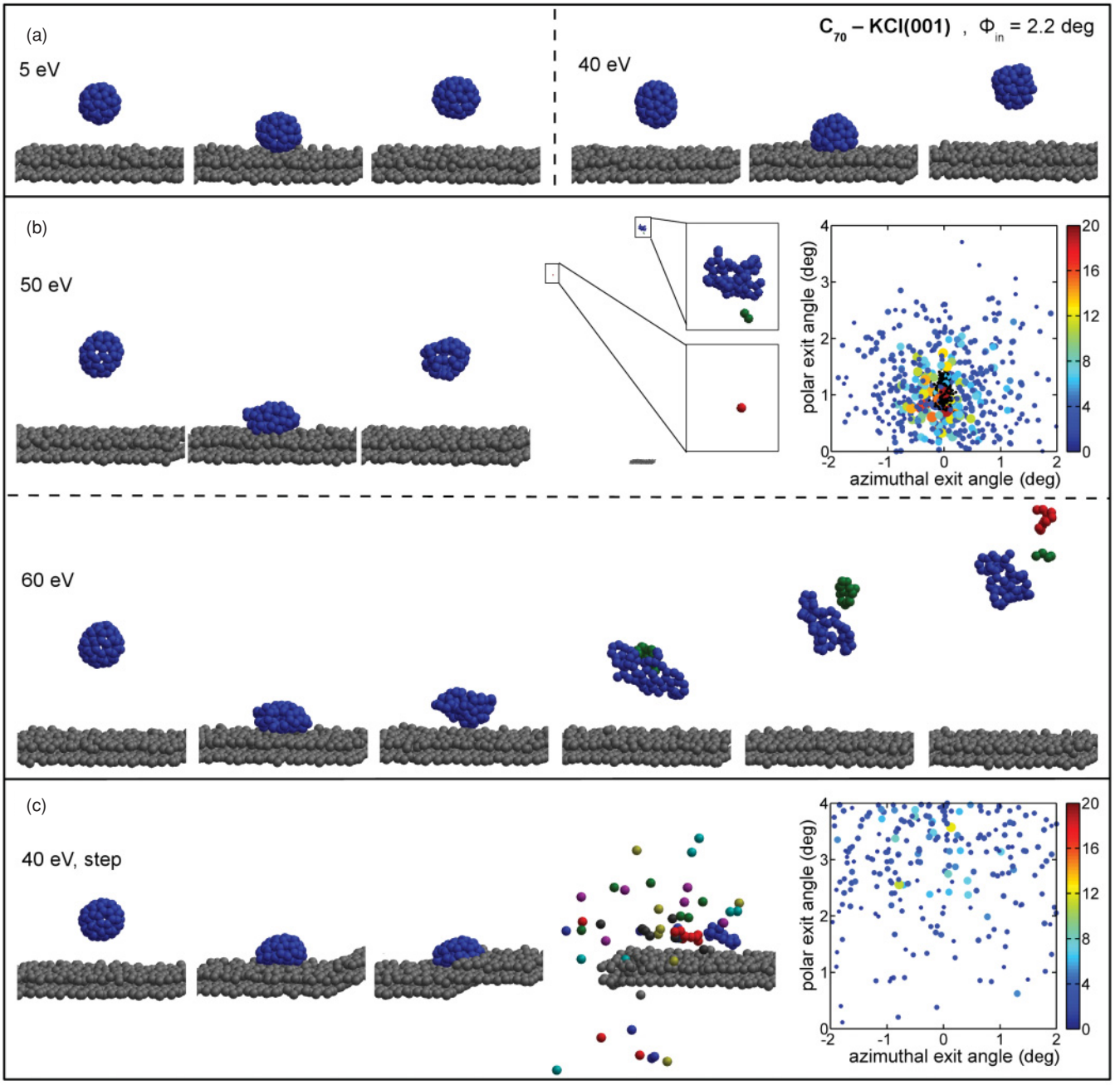

FIG. 10. (Color online) Snapshots from 3D trajectory calculations for C_{70} molecules scattered under a polar angle of incidence $\Phi_{in} = 2.2^\circ$ deg with indicated normal energies $E_\perp^{in}$ from a perfect KCl(001) surface (a, b) and a step on a KCl(001) surface (c). Insets: simulated impacts of fragments on the MCP detector without deflection plates. Fragment size encoded in size and color of points (color scale). Small black dots: impacts of large $C_{n>20}$ fragments. For details see text.

After surface impact, the fullerene atoms are followed for the characteristic electron detachment time of about 10^{-10} s.[47] If the molecule breaks apart during this time, that is, postcollision multifragmentation, the negative charge is assigned to one of the fragments, whereas the other fragments are neutral. Only one of these fragments will be detected, as the MCP detector is operated in a single-hit mode. If, after this time, all atoms of the fullerene still form an intact (defined by cutoff-radius of BOP) cluster, the electron is detached and a neutral particle is detected. In good accord with the analysis of the elastic properties of the fullerenes in Sec. III A, the negative ion fractions for normal energies $E_\perp \geqslant 30$ eV are reproduced by simulations based on the BOP by Erhart *et al.*[38] reduced by a factor of 0.75 (curves with open circles and squares in Fig. 9), whereas the negative ion fractions are strongly underestimated by the original BOP (curves with upward- and downward-pointing triangles in Fig. 9).

The reduced BOP also yields a quantitative reproduction of the size-integrated polar angular distributions of the small negative fragments $C^-_{n\leqslant 20}$ at normal energies $E_\perp \geqslant 30$ eV (see Fig. 11) as well as the tendency to broader angular distributions for smaller fragments [see inset in Fig. 8 and inset in

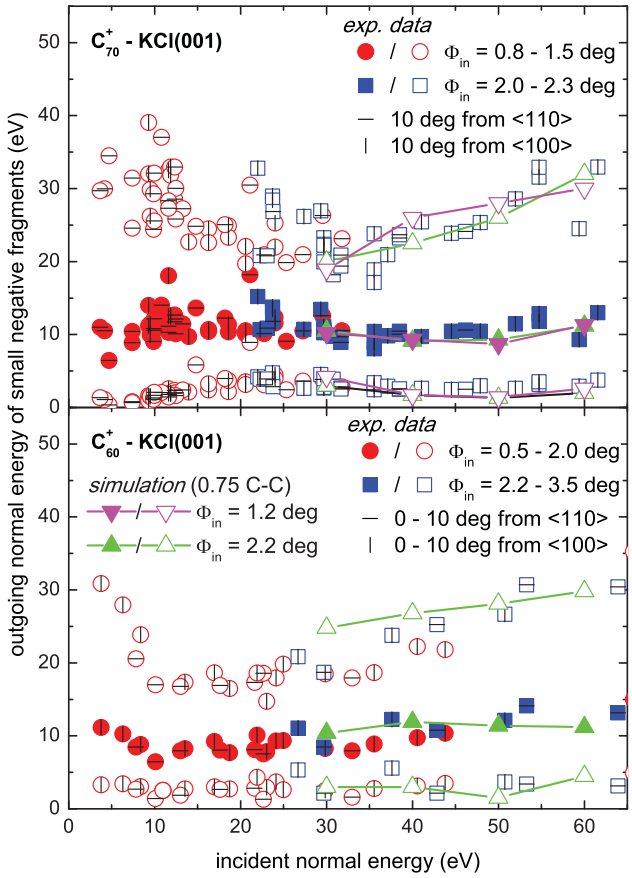

FIG. 11. (Color online) Outgoing normal energies $E_\perp^{\text{out}}$ from maxima (filled symbols) and half-maximum positions (open symbols) of size-integrated polar angular distributions of small negative $C^-_{n\leqslant 20}$ fragments as a function of incident normal energy $E_\perp^{\text{in}}$ for scattering of C_{70}^+ (upper panel) and C_{60}^+ molecules (lower panel) under the indicated angles of incidence Φ_{in} along the indicated azimuthal directions from a KCl(001) surface. Symbols: experimental data. Curves with symbols: results from 3D trajectory simulations for indicated parameters. For details see the text.

Fig. 10(b)]. Figure 11 compiles outgoing normal energies $E_\perp^{\text{out}}$ from maxima (filled symbols) and half-maximum positions (open symbols) of size-integrated polar angular distributions of the small negative $C^-_{n\leqslant 20}$ fragments as a function of incident normal energy $E_\perp^{\text{in}}$ for scattering of C_{70}^+ (upper panel) and C_{60}^+ molecules (lower panel) under indicated angles of incidence Φ_{in} along the indicated azimuthal directions from a KCl(001) surface. For normal energies $E_\perp \geqslant 30$ eV, measured (symbols) and simulated angular distributions for the reduced BOP (curves with symbols) agree on a quantitative level. At low normal energies $E_\perp \leqslant 20$ eV, the angular distributions for small negative fragments become very broad, as can be inferred from the comparison with the angular distributions for large clusters in Fig. 2. This, the angular dependence of the negative ion fractions in this region (see Fig. 9), and the ill-defined broad simulated angular distribution for scattering from a surface step in the inset in Fig. 10(c) are clear indications of fragment production at surface defects at low normal energies $E_\perp \leqslant$ 20 eV. However, due to the small negative ion fractions in this region (unlikely event) and he long trajectories for grazing scattering, this is still in accord with a good quality of the surface.

V. SUMMARY AND CONCLUSIONS

In summary, we have presented a comprehensive study of the interaction processes during grazing scattering of fast C_{70}^+ and C_{60}^+ molecules from a KCl(001) surface, with a focus on elasticity, internal excitation, fragmentation, and charge transfer. A similar behavior is observed for both fullerenes, which indicates that the results are not limited to a certain species but might be transferable to a wider class of carbon nanostructures.

At low energies for the motion along the surface normal of some electron volt, the molecules are reflected elastically, whereas at higher energies, the scattering is subspecular, with a slight dependence on the velocity of the motion parallel to the surface. From a comparison with classical 3D molecular dynamics simulations based on empirical bond order potentials for the carbon-carbon interaction by Tersoff[37] and Erhart *et al.*[38] and a number of different interaction potentials with the surface, we conclude that the bond order potentials do not reproduce the elastic properties of the fullerenes on a quantitative level. A reduction by a factor of 0.75 is needed to reproduce the experimental data, which was interpreted as a possible consequence of a kinematically assisted hybridization of fullerene and surface.[1,3,36]

The internal excitation of the fullerenes was deduced from the analysis of fragment size distributions due to delayed C_2^0 emission, where higher internal excitations are obtained for smaller grazing polar angles of incidence. A comparison with results from 3D trajectory simulations indicates the presence of an excitation mechanism not included in the simulations. Resonant coherent excitation of the molecule by the oscillating electric field of the surface experienced in the rest frame of the projectile,[1,22–25] which has recently been reported for scattering of C_{60} molecules from alkali-halide surfaces,[20,26,32] is a likely candidate here.

At low energies for the motion along the surface normal of about 1 eV, positive ion fractions close to 100% are observed, whereas toward higher energies, the positive ion fractions decrease exponentially with smaller values for molecules with a higher projectile velocity. As the highest-occupied molecular orbitals of the fullerenes are located about 0.5 eV above the valence band maximum of KCl(001),[8,34] a kinematically assisted one-electron transfer[1,36] might explain the experimental results.

As the electron detachment times of negatively charged fullerenes under our experimental conditions are too small to detect negatively charged fullerenes and the fullerenes exhibit high electron affinities,[8] the neutralization might as well be explained by a double-electron capture mechanism.[46] Furthermore, the internal excitation of ions is too high to produce stable negative fullerene ions. In the case of multifragmentation of the fullerene after the scattering process as recently reported by Kaplan *et al.*[16,17] for scattering of C_{60} under larger angles from a gold surface, the negative charge, however, can be detained by the small fragments. From our analysis of size distributions, fractions, and angular distributions for small, negatively charged $C^-_{n\leqslant 20}$ fragments, we conclude the first

observation of postcollision multifragmentation of fullerenes during grazing scattering from surfaces and deduce a threshold energy for the motion along the surface normal of about 20–30 eV. As in the case for the polar angular distributions, the analysis is in quantitative accord with 3D molecular dynamics simulations for empirical bond order potentials reduced by a factor of 0.75. Our results indicate a nearly complete conversion of the positively charged fullerenes to negative ions during scattering from the KCl(001) surface with energies for the motion along the surface normal of some 10 eV.

From this experimental study and the first attempts to develop theoretical models, we hope to trigger detailed theoretical investigations of the multifaceted aspects of this interesting model system of molecule surface interactions.

ACKNOWLEDGMENTS

Financial support by the Deutsche Forschungsgemeinschaft (DFG; Project No. Wi 1336) and fruitful discussions with K. Kimura (Kyoto), E. Kolodney (Haifa), and H. Zettergren and H. Cederquist (Stockholm) are gratefully acknowledged. We thank K. Maass, A. Schüller, and U. Specht (Berlin) for their assistance in the preparation of the experiments.

*mbusch@physik.hu-berlin.de

[1] H. Winter, Phys. Rep. **367**, 387 (2002).
[2] E. E. B. Campbell, *Fullerene Collision Reactions* (Kluwer Academic, London, 2003).
[3] F. Rosei, M. Schunack, Y. Naitoh, P. Jiang, A. Gourdon, E. Laegsgaard, I. Stensgaard, C. Joachim, and F. Besenbacher, Prog. Surf. Sci. **71**, 95 (2003).
[4] M. P. Anantram and F. Leonard, Rep. Prog. Phys. **69**, 507 (2006).
[5] J. Gauyacq, A. Borisov, and M. Bauer, Prog. Surf. Sci. **82**, 244 (2007).
[6] H. Brongersma, M. Draxler, M. de Ridder, and P. Bauer, Surf. Sci. Rep. **62**, 63 (2007).
[7] U. Bovensiepen, H. Petek, and M. Wolf, eds., *Dynamics at Solid State Surfaces and Interfaces* (Wiley-VCH, Weinheim, 2010).
[8] M. S. Dresselhaus, G. Dresselhaus, and P. C. Eklund, *Science of Fullerenes and Carbon Nanotubes* (Academic Press, San Diego, CA, 1996).
[9] R. H. Baughman, A. A. Zakhidov, and W. A. de Heer, Science **297**, 787 (2002).
[10] E. E. B. Campbell and F. Rohmund, Rep. Prog. Phys. **63**, 1061 (2000).
[11] M. Hillenkamp, J. Pfister, M. M. Kappes, and R. P. Webb, J. Chem. Phys. **111**, 10303 (1999).
[12] M. Hillenkamp, J. Pfister, and M. M. Kappes, J. Chem. Phys. **114**, 10457 (2001).
[13] E. Kolodney, B. Tsipinyuk, A. Bekkerman, and A. Budrevich, Nucl. Instrum. Methods Phys. Res., Sect. B **125**, 170 (1997).
[14] A. Bekkerman, B. Tsipinyuk, S. Verkhoturov, and E. Kolodney, J. Chem. Phys. **109**, 8652 (1998).
[15] A. Bekkerman, B. Tsipinyuk, and E. Kolodney, Phys. Rev. B **61**, 10463 (2000).
[16] A. Kaplan, A. Bekkerman, E. Gordon, B. Tsipinyuk, M. Fleischer, and E. Kolodney, Nucl. Instrum. Methods Phys. Res., Sect. B **232**, 184 (2005).
[17] A. Kaplan, A. Bekkerman, B. Tsipinyuk, and E. Kolodney, Phys. Rev. B **79**, 233405 (2009).
[18] D. S. Gemmell, Rev. Mod. Phys. **46**, 129 (1974).
[19] S. Tamehiro, T. Matsushita, K. Nakajima, M. Suzuki, and K. Kimura, Nucl. Instrum. Methods Phys. Res., Sect. B **256**, 16 (2007).
[20] T. Matsushita, K. Nakajima, M. Suzuki, and K. Kimura, Phys. Rev. A **76**, 032903 (2007).
[21] K. Kimura, T. Matsushita, K. Nakajima, and M. Suzuki, Nucl. Instrum. Methods Phys. Res., Sect. B **267**, 2638 (2009).
[22] V. V. Okorokov, JETP Lett. **2**, 111 (1965).
[23] K. Kimura, H. Ida, M. Fritz, and M. Mannami, Phys. Rev. Lett. **76**, 3850 (1996).
[24] C. Auth, A. Mertens, H. Winter, A. G. Borisov, and F. J. Garca de Abajo, Phys. Rev. Lett. **79**, 4477 (1997).
[25] T. Hecht and H. Winter, Phys. Lett. A **243**, 306 (1998).
[26] K. Kimura, private communication.
[27] S. Wethekam and H. Winter, Phys. Rev. A **76**, 032901 (2007).
[28] S. Wethekam, H. Winter, H. Cederquist, and H. Zettergren, Phys. Rev. Lett. **99**, 037601 (2007).
[29] S. Wethekam and H. Winter, Vacuum **82**, 895 (2008).
[30] S. Wethekam, H. Zettergren, C. Linsmeier, H. Cederquist, and H. Winter, Phys. Rev. B **81**, 121416 (2010).
[31] H. Zettergren, H. T. Schmidt, H. Cederquist, J. Jensen, S. Tomita, P. Hvelplund, H. Lebius, and B. A. Huber, Phys. Rev. A **66**, 032710 (2002).
[32] S. Wethekam and H. Winter, Nucl. Instr. Meth. Phys. Res. B (in press).
[33] R. Pfandzelter, Phys. Rev. B **57**, 15496 (1998).
[34] A. Goldmann and E. E. Koch, eds., *Landolt-Börnstein*, Vol. III 23a (Springer-Verlag, Berlin, 1989).
[35] Note that some values of KCl and KF have been interchanged in the tables in Ref. 34, as evident from the original publications.
[36] J. Los and J. J. C. Geerlings, Phys. Rep. **190**, 133(1990).
[37] J. Tersoff, Phys. Rev. Lett. **61**, 2879 (1988).
[38] P. Erhart and K. Albe, Phys. Rev. B **71**, 035211 (2005).
[39] D. J. O'Connor and J. P. Biersack, Nucl. Instrum. Methods Phys. Res., Sect. B **15**, 14 (1986).
[40] J. Vogt and H. Weiss, Surf. Sci. **491**, 155 (2001).
[41] S. Wethekam and H. Winter, Nucl. Instrum. Methods Phys. Res., Sect. B **258**, 48 (2007).
[42] A. J. Maxwell, P. A. Brühwiler, D. Arvanitis, J. Hasselström, M. K.-J. Johansson, and N. Mårtensson, Phys. Rev. B **57**, 7312 (1998).
[43] R. D. Beck, J. Rockenberger, P. Weis, and M. M. Kappes, J. Chem. Phys. **104**, 3638 (1996).
[44] R. T. Chancey, L. Oddershede, F. E. Harris, and J. R. Sabin, Phys. Rev. A **67**, 043203 (2003).
[45] B. Concina, S. Tomita, J. U. Andersen, and P. Hvelplund, Eur. Phys. J. D **34**, 191 (2005).
[46] P. Roncin, A. G. Borisov, H. Khemliche, A. Momeni, A. Mertens, and H. Winter, Phys. Rev. Lett. **89**, 043201 (2002).
[47] N. Walsh, A. Lassesson, F. Martinez, G. Marx, and L. Schweikhard, Vacuum **83**, 761 (2008).
[48] S. Yang, K. Taylor, M. Craycraft, J. Conceicao, C. Pettiette, O. Cheshnovsky, and R. Smalley, Chem. Phys. Lett. **144**, 431 (1988).